Available online at www.sciencedirect.com
ScienceDirect
Ceramics International 35 (2009) 2639–2644
CERAMICS INTERNATIONAL
www.elsevier.com/locate/ceramint

Thermal shock resistance and mechanical properties of $La_2Ce_2O_7$ thermal barrier coatings with segmented structure

Yi Wang [a,b], Hongbo Guo [a,b], Shengkai Gong [a,b,*]

[a] Beijing University of Aeronautics and Astronautics (BUAA), Department of Materials Science and Engineering, Xueyuan Road, No. 37, Beijing 100083, China
[b] Beijing Key Laboratory for Advanced Functional Materials and Thin Film Technology, BUAA, Beijing 100083, China

Received 3 November 2008; received in revised form 8 January 2009; accepted 28 February 2009
Available online 27 March 2009

Abstract

$La_2Ce_2O_7$ (LCO) is a promising candidate material for thermal barrier coatings (TBCs) application because of its higher temperature capability and better thermal insulation property relative to yttria stabilized zirconia (YSZ). In this work, $La_2Ce_2O_7$ TBC with segmentation crack structure was produced by atmospheric plasma spray (APS). The mechanical properties of the sprayed coatings at room temperature including microhardness, Young's modulus, fracture toughness and tensile strength were evaluated. The Young's modulus and microhardness of the segmented coating were measured to be about 25 and 5 GPa, relatively higher than those of the non-segmented coating, respectively. The fracture toughness of the LCO coating is in a range of 1.3–1.5 MPa $m^{1/2}$, about 40% lower than that of the YSZ coating. The segmented TBC had a lifetime of more than 700 cycles, improving the lifetime by nearly two times as compared to the non-segmented TBC. The failure of the segmented coating occurred by chipping spallation and delamination cracking within the coating.

Keywords: $La_2Ce_2O_7$ (LCO); Thermal barrier coatings (TBCs); Segmentation cracks; Thermal shock

1. Introduction

Plasma sprayed thermal barrier coatings (TBCs) have been extensively used in hot section components of gas turbines to protect the underlying components from exposing to high temperature gas. The selection of the TBC materials is restricted by some requirements such as low thermal conductivity, no phase transformation between room temperature and operation temperatures, high melting point and thermal expansion match with the underlying metallic substrate. Typical TBC systems are composed of ZrO_2 stabilized with 6–8 wt.%Y_2O_3 (YSZ) with a thickness of 200–250 μm. YSZ TBC could not long-term work at temperatures above 1523 K, due to the transformation of tetragonal phase to monoclinic phase. Such phase change, together with severe sintering at high temperature, accelerates the spallation failure of TBCs [1,2]. In the next generation of advanced engines, further increase in thrust-to-weight ratio will require even higher gas turbine inlet temperature (TIT). TBC materials with higher temperature capability and better thermal insulation performance than the current YSZ ceramic are in demand.

At present, some candidate materials for TBC application at higher temperature are under investigation, such as $LaMgAl_{11}O_{17}$, 7.5 mass% Y_2O_3–HfO_2 (YSH), $Gd_2Zr_2O_7$, $La_2Zr_2O_7$ and $La_2Ce_2O_7$ [3–5]. $La_2Ce_2O_7$ is a new candidate material for TBC because of its higher phase stability at 1673 K, lower thermal conductivity and larger thermal expansion coefficient than YSZ [6,7]. Partial decomposition of LCO occurs during plasma spraying or electron beam physical vapor deposition, due to different vapor pressures of La_2O_3 (8×10^{-5} atm, 2773 K) and CeO_2 (2×10^{-2} atm, 2773 K), which leads to composition derivation of the deposited LCO coating from the original LCO powders [8]. It is evident that such composition derivation certainly has negative effects on the properties of the sprayed materials. Thermal cycling lifetime of the plasma sprayed LCO TBC needs improvement in order to make fully use of the potential advantages of the coating. Recently, YSZ TBCs with high segmentation crack density sprayed at "hot

* Corresponding author at: Beijing University of Aeronautics and Astronautics (BUAA), Department of Materials Science and Engineering, Xueyuan Road, No. 37, Beijing 100083, China. Tel.: +86 10 8231 7117; fax: +86 10 8233 8200.
E-mail address: gongsk@buaa.edu.cn (S. Gong).

0272-8842/$36.00
doi:10.1016/j.ceramint.2009.02.025

condition'' have exhibited a promising potential in improving thermal shock resistance of TBCs, because the segmentation cracks formed in the TBC during the deposition significantly increase the strain tolerance of TBC [9].

In the present work, LCO TBCs are produced by plasma spray using various processing parameters, aiming at obtaining LCO coatings with nearly stoichiometric composition and segmented structure. Mechanical properties of the sprayed coatings including Young's modulus, hardness and fracture toughness are evaluated. Thermal shock resistance and associated failure mechanism of the LCO TBC are investigated.

2. Experimental procedures

2.1. Coating preparation

Powders used for synthesis of LCO included La_2O_3 (99.99%, Grirem Advanced Materials Co., Ltd., China) and CeO_2 (99.99%, Grirem Advanced Materials Co., Ltd., China). The details for the synthesis of LCO were described in the previous work [8]. Commercial NiCoCrAlY powders with a chemical composition of Ni–21Co–17Cr–12Al–1Y (in wt.%) were chosen for spraying the bond coats of TBCs. The LCO powders for spraying were produced by dried spraying technology and its morphology is shown in Fig. 1. The size of powders is in a range of 20–140 μm.

The LCO TBCs were produced by plasma spray with Sulzer Metco plasma spray units. Vacuum plasma spraying with an F4 gun was used to deposit a 50–80 μm NiCoCrAlY bond coat onto disk shaped Ni-based superalloy substrate. The substrate had a diameter of 25 mm and a thickness of 3 mm. The outer rim of the sample had a radius of curvature of 1.5 mm. LCO coatings were sprayed onto the NiCoCrAlY coated substrate by atmospheric plasma spraying. Segmentation cracks were generated by thermal tensile stresses during the deposition. The heat input to the substrate should be enough high to obtain a good bonding between lamellae which is necessary for propagation of vertical cracks from one lamellae to the next lamellae and finally to the coating surface [10]. Following these ideas, short spray distance, high plasma power and substrate preheating were used. The parameters used for spraying LCO coatings are listed in Table 1.

2.2. Evaluations of mechanical properties

Microhardness Knoop and Vickers indentations were performed on the cross-sections of the coatings using the HXZ-1000 microhardness indenter. The microhardness as well as the elastic modulus (E) of the coatings were determined by

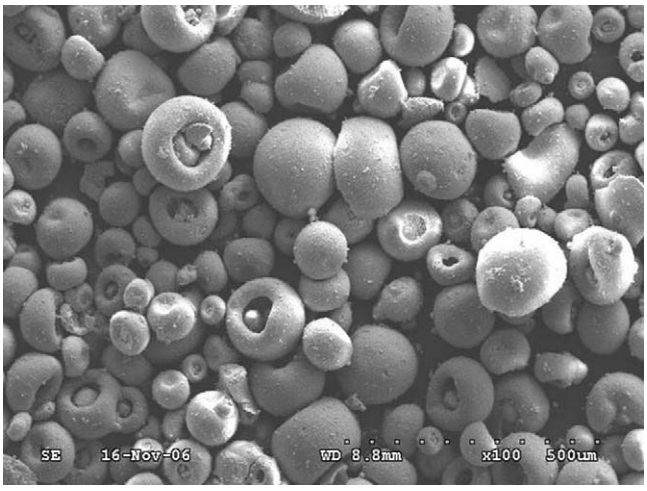

Fig. 1. Spray-dried powders for plasma spraying $La_2Ce_2O_7$ coating.

using the following equation [11,12]:

$$\frac{b'}{a'} = \frac{b}{a} - \frac{\alpha H_k}{E} \quad (1)$$

where b'/a' denotes the indent diagonal after elastic recovery during indentation; b/a is the ratio of the known Knoop indenter dimensions or geometry (1/7.11); α is a constant, having a value of 0.45; H_k is the Knoop microhardness value obtained from the indentation, while E is the Young's modulus of the coatings. Test load of 1.96 N with a holding time of 15 s was used in the investigation in accordance with ASTM E384.

The fracture toughness of the as-sprayed coatings was evaluated based on the equation shown below, which is related to the median cracks [13,14]:

$$K_{IC} = 0.016\left(\frac{E}{H_V}\right)^{1/2}\left(\frac{P}{C^{3/2}}\right) \quad (2)$$

where K_{IC} denotes the fracture toughness (MPa $m^{1/2}$); H_V the Vickers hardness (GPa); E the elastic modulus obtained from Eq. (1) (GPa); P the applied indentation load (kgf) and C is the radial crack length (mm).

The tensile adhesion test was performed using CMT5504 (SMS Co., Ltd., China) test machine. The coated stubs were adhesively glued together with coupling stubs using a cold-cured adhesive glue to investigate the mechanical bond strength. The crosshead speed used was 1 mm/min.

2.3. Thermal shock test

Thermal shock testing was performed in a gas burner test facility. The sample was heated for 20 s to the desire surface temperature of 1523 K and then held at this temperature for

Table 1
Processing parameters for spraying $La_2Ce_2O_7$ coatings.

Coating	Power (kW)	Distance (mm)	Ar (slpm)/H_2 (slpm)	Feed rate (g/min)	Gun velocity (mm/s)
a	40.2	70	45/10	35	500
b	45	60	45/12	35	500

5 min. During the heating the backside of the sample was cooled by compressed air to maintain a controlled temperature gradient through the sample and in this case, the temperature of substrate was in the range 1223–1273 K. After finishing the heating the burner was removed automatically from the coating surface and the sample was cooled for 2 min. The lifetime of the coating is defined as the number of thermal cycles at which spallation area of the coating is more than 20% of the surface area of the coating.

2.4. Microstructure characterization

The sprayed samples were impregnated with epoxy and then sectioned, ground and polished. The planar section and cross-section of the coatings were examined by optical microscope (OM) and scanning electron microscope (SEM), the compositions of the coatings analyzed by energy dispersive spectroscopy (EDS). Segmentation crack density was defined as the number of segmentation cracks in a cross-section of coating divided by the length of cross-section.

3. Results and discussion

3.1. Microstructure and phase of sprayed LCO coatings

Fig. 2a and b shows SEM micrographs of cross-sections of sprayed LCO coatings with spray set number a and b as listed in Table 1, respectively. Coating a reveals a typical lamellar structure, with a LCO coating thickness of around 100 μm. In contrast to coating a, coating b contains several segmentation cracks which went through the LCO coating thickness. The segmentation crack density was measured to be 9.5 mm^{-1}. Besides, some branching cracks were present together with the segmentation cracks.

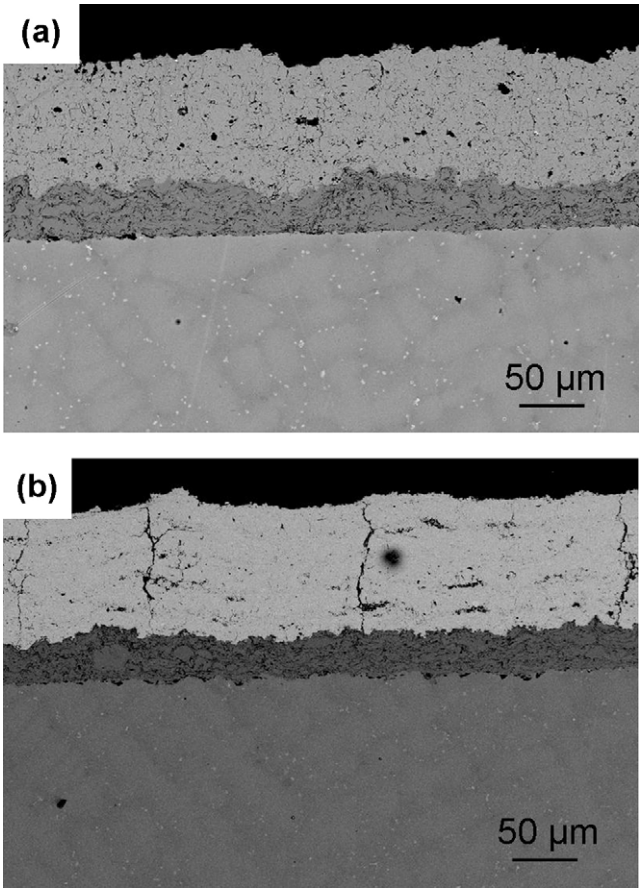

Fig. 2. SEM micrographs of cross-sections of the sprayed LCO coatings sprayed at conditions (a and b), respectively.

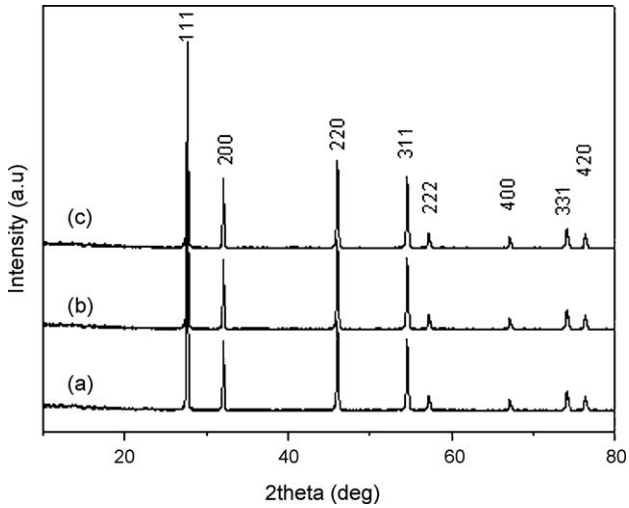

Fig. 3. XRD patterns of the LCO powders (a), the non-segmented LCO coating (b) and the segmented LCO coating (c).

Fig. 3 shows XRD patterns of the LCO powders and the sprayed coatings, respectively. The LCO coatings remained single $La_2Ce_2O_7$ phase and no decomposition occurred after plasma spraying. The chemical compositions of the sprayed coatings determined by EDS are given in Table 2. Both coatings have a chemical composition closed to the stoichiometric composition of $La_2Ce_2O_7$; despite there is a little derivation in the composition. This indicates that the single LCO coatings with a nearly stoichiometric composition were obtained under the present plasma spray conditions.

Partial decomposition of LCO usually occurs during plasma spraying or electron beam physical vapor deposition, due to different vapor pressures of La_2O_3 (8×10^{-5} atm, 2773 K) and CeO_2 (2×10^{-2} atm, 2773 K), which leads to composition derivation of the deposited LCO coating from the original LCO powders. In viewing of this, it is necessary to consider the design of chemical composition of original powders, in order to obtain the sprayed LCO coating with nearly stoichiometric composition and single LCO phase. Usually, the segmented ceramic coatings were produced at "hot" spray conditions. Under "hot" spray condition, a good lamellar bonding was achieved so that vertical cracks could propagate from one lamellae to another lamellae and finally develop into segmentation cracks.

Table 2
Compositions of sprayed LCO coatings (in at.%).

Coating	La	Ce	O
a	21.85	20.08	58.08
b	23.99	20.52	55.49

3.2. Thermal shock performance

The sprayed coatings including the segmented one and the non-segmented one were subjected to thermal shock testing, in which the coated samples were heated for 20 s to the maximum temperature of around 1523 K and held at this temperature for 5 min and then cooled down by compressed air. During the heating stage, the backside temperature (substrate temperature) ranged from 1223 to 1273 K. The segmented sample exhibited a lifetime of more than 700 cycles, while spallation failure of the non-segmented sample occurred after around 200 cycles, as shown in Fig. 4. The lifetime of the segmented TBC is nearly three times that of the non-segmented TBC. This indicates that the LCO TBC with segmentation cracks significantly improved thermal shock resistance, as compared to the TBC without segmentation cracks. Fig. 5 shows a photograph of the segmented TBC sample after 730 thermal cycles. Spallation failure is visible along the sample rim, which is usually a failure mechanism for TBC due to the singularity of thermal stresses at the rim. The sample was sectioned along the black line as marked in Fig. 5 for cross-section analysis. Fig. 6a and b shows the cross-sections of the center area and the rim area of the sample, respectively. In the center area, the LCO coating became thinner than the as-sprayed coating due to chipping spallation during thermal shock testing, which is reported to be a typical failure for segmented TBCs [10]. However, in the rim area, spallation caused by delamination cracking occurred, which is a usual failure mode for plasma sprayed TBCs. It should be noted that oxidation of bond coat did not dominate the thermal cycling lifetime, since the substrate temperature is not high enough and oxidation time not long enough to form a thick TGO layer.

Spallation failure of plasma sprayed TBCs occurs in most cases by delamination cracking at the interface between the first lamellae and the adjacent lamellae. Segmentation cracks in TBCs tend to lower the strain energy for cracking and greatly improve the strain tolerance of the TBC in a manner, which behaves like the columnar structure in PVD coatings. Therefore, the segmented TBCs have exhibited a prolonged thermal cycling lifetime as compared to the non-segmented TBCs.

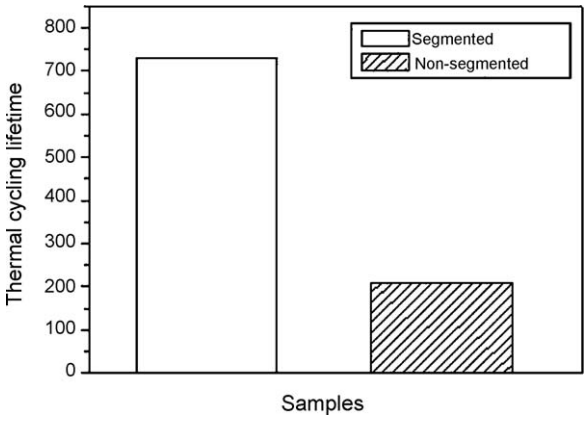

Fig. 4. Thermal cycling lifetime of LCO TBCs.

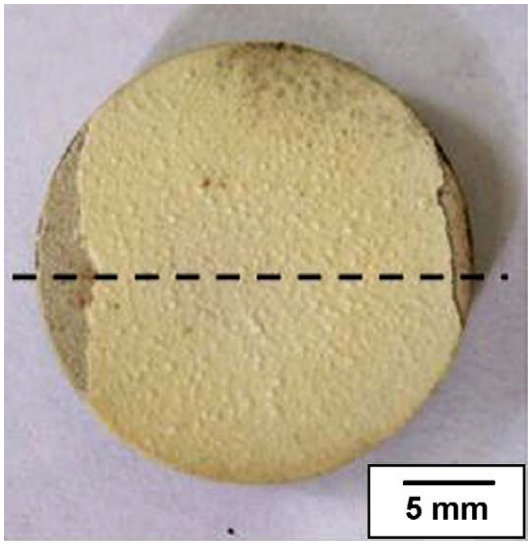

Fig. 5. Photograph of the Segmented LCO TBC sample after 730 thermal cycles.

3.3. Mechanical properties

Coatings a and b as shown in Fig. 2 were chosen for evaluation of mechanical properties. An average of 15 indentations along the cross-section of the coatings was taken for 5 sets of each sample. To avoid indentation size effect, the highest possible indentation load, which did not cause cracking, was used. The values of microhardness and the Young's modulus determined in Eq. (1) are given in Fig. 7a and b, respectively. The microhardness decreases with increasing indentation load and approaches a steady state value under an indentation load of 1.96 N. For the segmented sample, the microhardness is measured to be around 5 GPa and the Young's

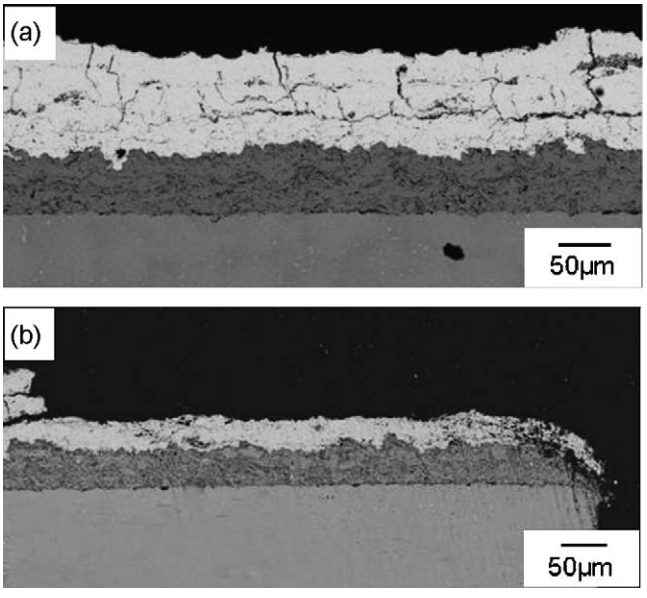

Fig. 6. SEM micrographs of cross-sections of the sprayed LCO TBC sample after 730 cycles, where (a) and (b) were sectioned from the center area and the rim area along the black line as marked in Fig. 5, respectively.

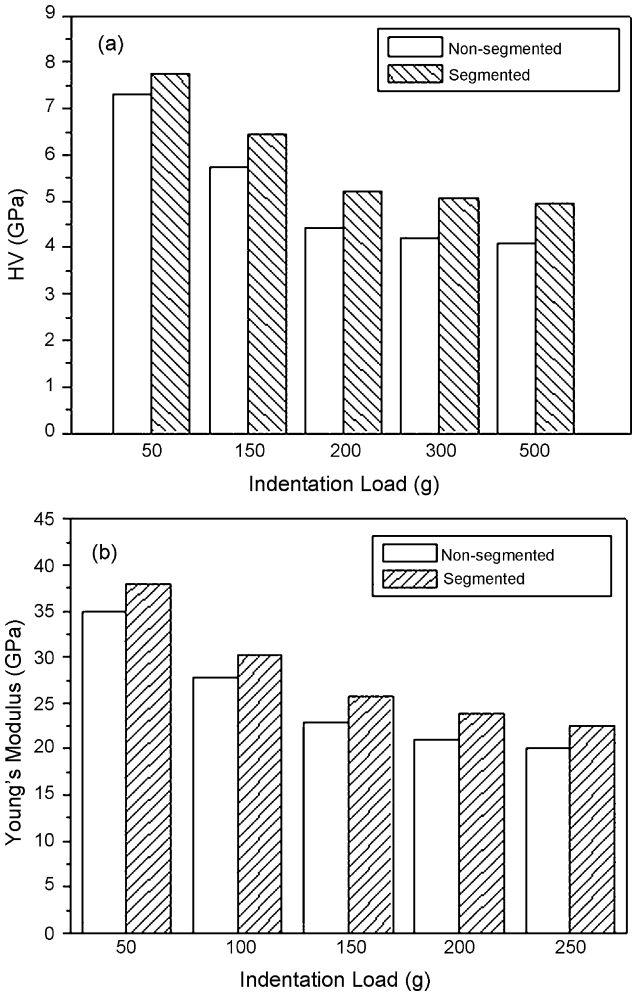

Fig. 7. Microhardness (a) and Young's modulus (b) of LCO coatings.

modulus is determined to be 25 GPa. Compared to the non-segmented coating, the segmented coating reveals relatively higher values of the mechanical properties, which is related to its microstructure features. It is well admitted that the segmented coatings are usually featured with lower porosity and good lamellar bonding due to its "hot" spray condition [9]. The lower porosity and better lamellar bonding of the segmented coating could be responsible for the improvement in the mechanical properties.

Fracture toughness of the LCO coating was determined at an indentation load of 4.9 N. The average value of the LCO coating is in a range of 1.3–1.5 MPa $m^{1/2}$ (as shown in Fig. 8), which is about 40% lower than that of the YSZ coating [15]. To sustain a satisfying thermal cycling performance, high fracture toughness is promising for TBC materials. YSZ has higher fracture toughness than most of TBC candidates partially due to its phase transformation toughening mechanism. Considering this, a LCO/YSZ double ceramic-layered structure was proposed, where the YSZ was used as the bottom layer to balance with the underlying metallic part in TBC system and endure larger impact of strain energy during thermal cycling.

Tensile strength, which is a measure of the adhesion ability of the coating to the substrate, is an important property of thermal-

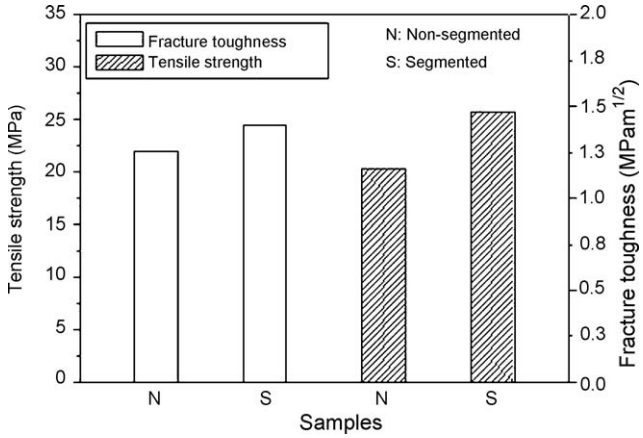

Fig. 8. Fracture toughness and tensile strength of LCO coatings.

sprayed coatings. In the present study, the tensile test was performed on the as-sprayed coatings. An average value of 25.8 MPa was achieved in the segmented coating, while the non-segmented coating yielded a tensile strength of around 20.3 MPa. For the two coatings, delamination cracking occurred within the LCO layer rather than at the interface between the ceramic layer and the MCrAlY layer. In terms of the tensile test results, it can be concluded that the segmented coating has an enhanced lamellar bonding. During "hot" spraying condition, high heat input to the substrate led to a higher substrate temperature that could promote the joining of adjacent lamellae.

4. Conclusions

The LCO thermal barrier coating containing segmentation cracks was produced under "hot" spray condition, while remaining phase stability and nearly stoichiometric composition. The segmentation crack density was measured to be around 9.5 mm^{-1}. The segmented TBC exhibited a thermal cycling lifetime of around 700 cycles, improving the lifetime by nearly two times as compared to the non-segmented TBC. The failure of the segmented coating occurred by chipping spallation and delamination cracking within the coating. The mechanical properties of the LCO TBC were evaluated. The microhardness and Young's modulus for the segmented coating was measured to be around 5 and 25 GPa, relatively higher than those of the non-segmented coating, respectively. The fracture toughness of the LCO coating is in a range of 1.3–1.5 MPa $m^{1/2}$, which was about 40% lower than that of the YSZ.

Acknowledgements

This research is sponsored by National Natural Science Foundation of China (NSFC nos. 50771009 and 50731001) and program for Changjiang Scholars and Innovative Research Team in University (PCSIRT) (IRT0512).

References

[1] R. Vassen, F. Tietz, G. Kerkhoff, et al., New materials for advanced thermal barrier coatings, in: Proceedings of the 6th Liege Conference on

Materials for Advanced Power Engineering, Universite de Liege, Belgium, (1998), pp. 1627–1635.
[2] R.A. Milller, Thermal barrier coatings for aircraft engines: history and directions, J. Therm. Spray Technol. 6 (1) (1997) 35–42.
[3] X.Q. Cao, R. Vassen, D. Stoever, Ceramic materials for thermal barrier coatings, J. Eur. Ceram. Soc. 24 (2004) 1–10.
[4] J. Wu, Novel Low-thermal Conductivity Ceramics for Thermal Barrier Coating, University of Connecticut, USA, 2004.
[5] K. Matsumoto, Y. Itoh, T. Kameda, EB-PVD process and thermal properties of Hafnia-based thermal barrier coating, Sci. Technol. Adv. Mater. 4 (2003) 153–158.
[6] W. Ma, S. Gong, H. Xu, On improving the phase stability and thermal expansion coefficients of lanthanum cerium oxide solid solutions, Scripta Mater. 54 (2006) 1505–1508.
[7] X.Q. Cao, R. Vassen, W. Jungen, S. Schwartz, F. Tietz, D. Stover, Thermal stability of lanthanum zirconate plasma-sprayed coating, J. Am. Ceram. Soc. 84 (2001) 2086–2090.
[8] W. Ma, S. Gong, H. Xu, et al., The thermal cycling behavior of lanthanum–cerium oxide thermal barrier coating prepared by EB-PVD, Surf. Coat. Technol. 200 (2006) 5113–5118.
[9] H.B. Guo, H. Murakami, S. Kuroda, Effect of hollow spherical powder size distribution on porosity and segmentation cracks in thermal barrier coatings, J. Am. Ceram. Soc. 89 (2006) 3797–3804.
[10] H.B. Guo, S. Kuroda, H. Murakami, Segmented thermal barrier coatings produced by atmospheric plasma spraying hollow powders, Thin Solid Films 506–507 (2006) 136–139.
[11] K.A. Khor, Y.W. Gu, C.H. Quek, P. Cheang, Plasma spraying of functionally graded hydroxyapatite/Ti–6Al–4V coatings, Surf. Coat. Technol. 168 (2003) 195–201.
[12] S.W.K. Kweh, K.A. Khor, P. Cheang, Plasma-sprayed hydroxyapatite (HA) coatings with flame-spheroidized feedstock: microstructure and mechanical properties, Biomaterials 21 (2000) 1223–1234.
[13] G. Bolelli, V. Cannillo, L. Lusvarghi, Plasma-sprayed glass–ceramic coatings on ceramic tiles: microstructure, chemical resistance and mechanical properties, J. Eur. Ceram. Soc. 25 (2005) 1835–1853.
[14] F.A. Costa Oliveiraa, J. Cruz Fernandes, Mechanical and thermal behaviour of cordierite–zirconia composites, Ceram. Int. 28 (2002) 79–91.
[15] R. Taylor, J.R. Brandon, P. Morrell, Microstructure, composition and property relationships of plasma-sprayed thermal barrier coatings, Surf. Coat. Technol. 50 (1992) 141–149.